Protection and Fault Locating Method of Series Compensated Lines by Wavelet Based Energy Traveling Wave

Yu Liu, *Student Member, IEEE*; Sakis Meliopoulos, *Fellow, IEEE*; Nengling Tai, *Member, IEEE*; Liangyi Sun, *Student Member, IEEE* and Boqi Xie, *Student Member, IEEE*

Abstract: Series capacitors (SCs) in transmission lines increase the complexity of transmission line protection. In this paper, a wavelet based energy traveling wave protection and fault locating method for series compensated transmission lines is proposed. The method requires GPS synchronized measurements at both ends of the line. The paper first presents the propagation properties of transient currents with different frequency, and then a proper frequency band condition is generated to minimize the transient attenuation. The method uses energy traveling wave in certain frequency band extracted by wavelet transform, and the wavefront time difference of two measurement units at each end of transmission line is introduced for the purpose of executing tripping logic and computing fault location. Numerical simulations verify that the method provides a robust protection criterion and an accurate fault locating method, independently of type, fault impedances and locations along the line. The algorithm also works for different SCs locations, and it is not influenced by MOV/air gap operation.

Key words: Series Capacitors (SCs), transmission line protection, Metal Oxide Varistor (MOV), wavelet transform, energy traveling wave.

I INTRODUCTION

SERIES Capacitors (SCs) can improve stability of power system, increase transmission capability, reduce losses and damp sub-synchronous oscillations. The presence of SCs changes the continuity of the line inductive impedance and creates protection problems such as voltage/current inversion [1-2]. Moreover, the operation of the Metal Oxide Varistors (MOVs) and the air gap may change the compensation ratio of the line and generate additional transients, causing additional protection problems [3-4].

In the transmission system of Fig. 1, SCs are located at M side of transmission line MN. Overcurrent protection, distance protection and directional elements will all confront some issues. Fault F_1 may cause mis-operation of overcurrent protection and distance protection at relay I, because SCs reduce the impedance between F_1 and relay I; to prevent relay I from overreaching, the protection zone should be shortened. Additionally, with the fault at F_2, directional element at relay II may fail to operate, while directional elements at relay III and IV may mis-operate, due to capacitive impedance between F_2 and relay II.

Enabled by communications between two ends, pilot protection of transmission lines is usually more reliable than single-ended protection. However, phase/direction comparison protection, pilot distance protection and line differential protection still have their own limitations in series compensated transmission line. First, phase/direction comparison protection may fail during fault F_2, since directional elements at relay II may "see" a current in reverse direction. Second, pilot distance protection may fail to trip fault F_2, since the shortened protection zone of relay I will not "see" fault F_2, and relay II may wrongly consider it as an external fault. Moreover, the widely adopted line differential protection also has its own problems due to distributed capacitances, current inversion and limited sensitivity during high impedance faults [5].

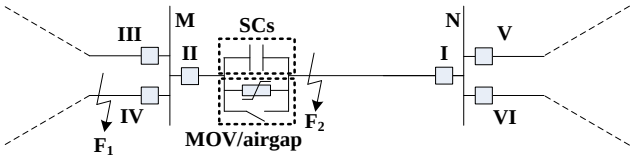

Fig. 1. Transmission system with SCs

Many attempts have been made to address these issues of series compensated line protection. Girgis et al [6] proposed a Kalman and adaptive Kalman filtering approach. This method is based on the assumption that SCs will be bypassed during fault, which is not strictly correct since some internal faults with lower fault current may not trigger MOV or air gap operation. Fault section methods [7-8], which identify whether SCs exist in the fault loop, are proposed to calculate fault location by considering the impedance of SCs. These approaches do not consider the uncertainty of the SC block (SCs, MOV, air gap) reactance due to nonlinear V-I characteristics of MOV as well as the air gap. Pattern classification and feature extraction has been also proposed to determine the fault location via neural network-based procedures [9-10]. These methods are sensitive to system changes, and require large training sets and long training time.

Transient traveling waves contain plenty of information and can be used in analyzing and locating the fault [11-12]. Nevertheless, recent methods rarely consider the attenuation of the traveling wave. In fact, since the traveling wave is a broad-band signal, its attenuation properties as transmitting /reflecting at each discontinuity of the line (faults, series capacitors, buses, etc.) are different for different frequency components. Consequently, in order to increase the accuracy of wavefront detection, the paper extracts the transient signal in a proper frequency band. Wavelet transform has been widely used in power systems to analyze transient signals, extract characteristics on different frequency bands, and capture

Yu Liu, Sakis. Meliopoulos, Liangyi Sun and Boqi Xie are with the School of Electrical and Computer Engineering, Georgia Institute of Technology, Atlanta, GA 30332 USA (e-mail: yliu400@gatech.edu, sakis.m@gatech.edu, lsun30@gatech.edu, airxbq@gatech.edu).

Nengling Tai is with Shanghai Jiao Tong University, Shanghai, 200240 China (e-mail: nltai@sjtu.edu.cn).

features of propagating waves on transmission lines due to its multi-resolution capability. The modulus maxima of wavelet transform can detect sharp variations of signal [13-15] which is very useful to precisely locating the wavefront.

In this paper, wavelet transform is used to extract traveling waves in certain frequency band. The time difference between the arrival of the first wavefront at both ends of the transmission line is introduced to determine fault location and enable trip decision. Numerical simulation results are provided to demonstrate the effectiveness of this algorithm.

II Propagation Properties of Traveling Waves

When a fault occurs, high frequency broad-band traveling waves are generated and propagate along the transmission line. At each discontinuity, the traveling waves partially reflect and partially transmit generating more traveling waves. The fault location can be calculated by detecting the first wavefront arrival time of traveling waves (usually current traveling waves) at both ends of the transmission line. The accuracy of this fault locating method largely depends on the accuracy of the wavefront detection. Bus capacitance and the transmission line series capacitance influence the attenuation of traveling waves and make the detection of the wavefront challenging. The accuracy of traditional traveling wave algorithms may be compromised. In this section, we will analyze the effects of SCs and bus capacitance on different frequency components of current traveling waves, from which we can find a proper frequency band that enables higher accuracy detection of the wavefront via wavelet transforms.

Fig. 2 shows a typical system with SCs. It includes buses P, M, N and Q with bus capacitance C_s. There are 3 transmission lines PM, MN and NQ with surge impedances Z_2, Z_1 and Z_3, respectively. Bus M and N also have branches with equivalent surge impedances $Z_{2\Sigma}$ and $Z_{3\Sigma}$, respectively. SCs with capacitance C are installed in transmission line MN.

Here series resistance and shunt conductance are neglectable compared to series reactance and shunt susceptance of the transmission line. Also, distributed capacitance C_{Line} and inductance L_{Line} are approximately constant, which results in a constant surge impedance $\sqrt{L_{Line}/C_{Line}}$.

Next, we will analyze the criterion of a proper frequency band to minimize current traveling wave attenuation along the line. Here four possible fault locations F_1~F_4 are considered. The current traveling waves are measured at the location of relay I and II.

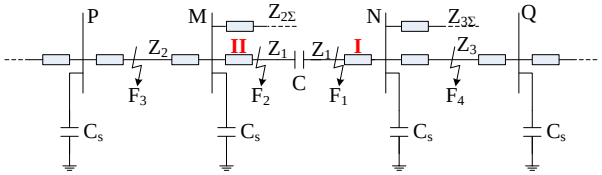

Fig.2 Transmission line system with SCs

A. Reflection and Refraction of Fault Current Transients

Reflection and refraction properties of fault current transients with frequency *f* are assessed below.

1) At SCs, the input surge impedance is Z_1, and the output surge impedance is $Z_1 + 1/j2\pi fC$.

Current wave refraction coefficient is,

$$\alpha_T(f) = \frac{2Z_1}{Z_1 + (Z_1 + 1/j2\pi fC)} = \frac{j4\pi fCZ_1}{1 + j4\pi fCZ_1} \tag{1}$$

Current wave reflection coefficient is,

$$\beta_N(f) = \frac{Z_1 - (Z_1 + 1/j2\pi fC)}{Z_1 + (Z_1 + 1/j2\pi fC)} = \frac{-1}{1 + j4\pi fCZ_1} \tag{2}$$

The current ratio between output and input current at SCs is,

$$\gamma_T(f) = \alpha_T(f) = j4\pi fCZ_1 / (1 + j4\pi fCZ_1) \tag{3}$$

2) At bus M with bus capacitance C_s, for the current wave traveling from PM to MN, the input surge impedance is Z_2, and the output surge impedance is $Z_1 \,||\, (1/j2\pi fC_s) \,||\, Z_{2\Sigma}$.

Current wave refraction coefficient is,

$$\begin{aligned}\alpha_{Ts,M}(f) &= \frac{2Z_2}{Z_1 \,||\, (1/j2\pi fC_s) \,||\, Z_{2\Sigma} + Z_2} \\ &= \frac{2Z_1Z_2 + 2Z_2Z_{2\Sigma} + 4Z_1Z_2Z_{2\Sigma} j\pi fC_s}{Z_1Z_2 + Z_2Z_{2\Sigma} + Z_1Z_{2\Sigma} + 2Z_1Z_2Z_{2\Sigma} j\pi fC_s}\end{aligned} \tag{4}$$

Current wave reflection coefficient is,

$$\begin{aligned}\beta_{Ns,M}(f) &= \frac{Z_2 - Z_1 \,||\, (1/j2\pi fC_s) \,||\, Z_{2\Sigma}}{Z_2 + Z_1 \,||\, (1/j2\pi fC_s) \,||\, Z_{2\Sigma}} \\ &= \frac{2Z_1Z_2Z_{2\Sigma} j\pi fC_s + Z_1Z_2 + Z_2Z_{2\Sigma} - Z_1Z_{2\Sigma}}{2Z_1Z_2Z_{2\Sigma} j\pi fC_s + Z_1Z_2 + Z_2Z_{2\Sigma} + Z_1Z_{2\Sigma}}\end{aligned} \tag{5}$$

The current ratio between the output and input current traveling wave at bus M is,

$$\begin{aligned}\gamma_{Ts,M}(f) &= \alpha_{Ts,M}(f) \times \frac{Z_{2\Sigma} \,||\, (1/j2\pi fC_s)}{Z_1 + Z_{2\Sigma} \,||\, (1/j2\pi fC_s)} \\ &= \frac{2Z_2Z_{2\Sigma}}{Z_1Z_2 + Z_2Z_{2\Sigma} + Z_1Z_{2\Sigma} + 2Z_1Z_2Z_{2\Sigma} j\pi fC_s}\end{aligned} \tag{6}$$

3) At bus N with bus capacitance C_s, for the current wave traveling from QN to NM, similarly, the current ratio between the output and input current traveling wave is,

$$\gamma_{Ts,N}(f) = \frac{2Z_3Z_{3\Sigma}}{Z_1Z_3 + Z_3Z_{3\Sigma} + Z_1Z_{3\Sigma} + 2Z_1Z_3Z_{3\Sigma} j\pi fC_s} \tag{7}$$

B. Proper Frequency Band Condition

Consider relay I in Fig. 2 as an example. Four possible fault locations F_1~F_4 were considered to investigate the characteristics of waves with specific frequency *f*.

1) If fault occurs at F_1, the current traveling wave will not be influenced by neither SCs nor bus capacitance.

2) If fault occurs at F_2, the current traveling wave will be attenuated by SCs. In order to identify a proper energy frequency band to accurately detect the first wavefront, we should let,

$$\gamma_T(f) \approx 1 \tag{8}$$

3) If fault occurs at F_3, the current traveling wave will be attenuated by both the bus capacitance at bus M and SCs. We

should let,

$$\gamma_T(f)\cdot\gamma_{Ts,M}(f)\approx 1 \tag{9}$$

4) If fault occurs at F_4, the current traveling wave will be attenuated by the bus capacitance at bus N. We should let,

$$\gamma_{Ts,N}(f)\approx 1 \tag{10}$$

From equation (3), (6), (8), (9) and (10), we get the proper frequency band condition,

$$1/(4\pi CZ_1)\ll f\ll f_{\max} \tag{11}$$

where

$$f_{\max}=\min\left(\frac{Z_1Z_2+Z_2Z_{2\Sigma}+Z_1Z_{2\Sigma}}{2\pi Z_1Z_2Z_{2\Sigma}C_s},\frac{Z_1Z_3+Z_3Z_{3\Sigma}+Z_1Z_{3\Sigma}}{2\pi Z_1Z_3Z_{3\Sigma}C_s}\right) \tag{12}$$

Similarly, relay II can also derive the same conclusion as relay I.

In summary, if the condition above is satisfied, the current traveling wave attenuation along the line will be relatively small. The detection is designed to focus on this frequency band of the traveling wave to obtain the best sensitivity in determining the fault location, which in turn will improve line protection.

III Wavelet Transform

The first application of wavelet transform is to effectively extract proper frequency band selected in Section II. The input signal passes through a high pass filter and a low pass filter respectively, suffers a down sampling, and produces detail coefficient (D_i) as well as approximate coefficient (A_i), corresponding to different frequency band. Continue this process with A_i to generate D_{i+1} and A_{i+1} ($i=1, 2,\cdots$), as illustrated in Fig. 3. After calculating corresponding coefficients, we can reconstruct the waveform to obtain transient wave in specific frequency band.

The second application of wavelet transform is to reliably capture sharp variations of signal by the modulus maxima. This feature is used to detect the wavefront of the traveling wave.

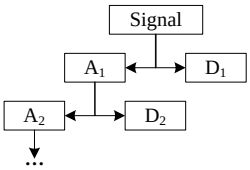

Fig. 3 Process of extracting frequency band by wavelet transform

IV Proposed Algorithm

We propose the use of an energy traveling wave algorithm which provides very good sensitivity. Energy traveling wave is a calculated energy sequence of a signal, where each energy point is obtained within the energy calculation time t_{energy}. Fig. 4 demonstrates this process with sampling frequency f_s. Here the current measurements at both ends of the transmission line were used. Define energy calculation time as t_{energy}; 3-phase currents at both ends as $i_{1,a}$, $i_{1,b}$, $i_{1,c}$, $i_{2,a}$, $i_{2,b}$ and $i_{2,c}$. Thus, the energy calculation data at time t contain 6 current sequences, $i_{1,a}^{(t)}$, $i_{1,b}^{(t)}$, $i_{1,c}^{(t)}$, $i_{2,a}^{(t)}$, $i_{2,b}^{(t)}$ and $i_{2,c}^{(t)}$, with $t_{\text{energy}}\times f_s$ sampling points each.

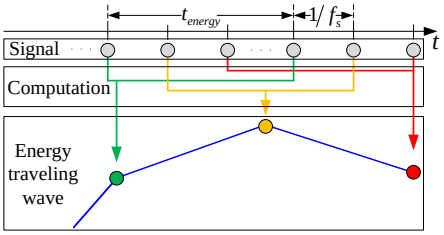

Fig. 4 Calculation of energy traveling wave

To calculate the value of the energy traveling wave (energy point) at time t , formulate mode current as follows,

$$i_{j,\text{mode}}^{(t)}=i_{j,a}^{(t)}+2i_{j,b}^{(t)}-3i_{j,c}^{(t)}\quad(j=1,2) \tag{13}$$

After that, adopt normalization for computed current,

$$i_{j,\text{norm}}^{(t)}(n)=i_{j,\text{mode}}^{(t)}(n)\Big/\left\|i_{j,\text{mode}}^{(t)}\right\|_2\quad(j=1,2) \tag{14}$$

where n is set to be integers from $1\sim(t_{\text{energy}}\times f_s)$.

Here we choose orthogonal, biorthogonal Daubechies 5 wavelet and use wavelet transform to calculate detail coefficient and reconstruct high frequency signal $D_j^{(t)}$ with band mentioned in equation (11). Subsequently, we calculate corresponding energy $E_{j,D}^{(t)}$.

$$E_{j,D}^{(t)}=\sum_{i=1}^{t_{\text{energy}}\times f_s}\left|D_j^{(t)}(i)\right|^2\quad(j=1,2) \tag{15}$$

Finally, after formulating energy traveling waves at both ends, capture the wavefront time T_1 and T_2 by the modulus maxima of wavelet transform, and compute time differences $\Delta T=T_1-T_2$. The relay should operate if,

$$|\Delta T|<l/v \tag{16}$$

where l is the length of the monitored transmission line, and v is the speed of traveling wave.

The distance between side 1 and fault location d_{1f} is,

$$d_{1f}=(l+v\cdot\Delta T)/2 \tag{17}$$

Fig. 5 shows time-domain calculation process of this algorithm, where $\Delta t=1/f_s$.

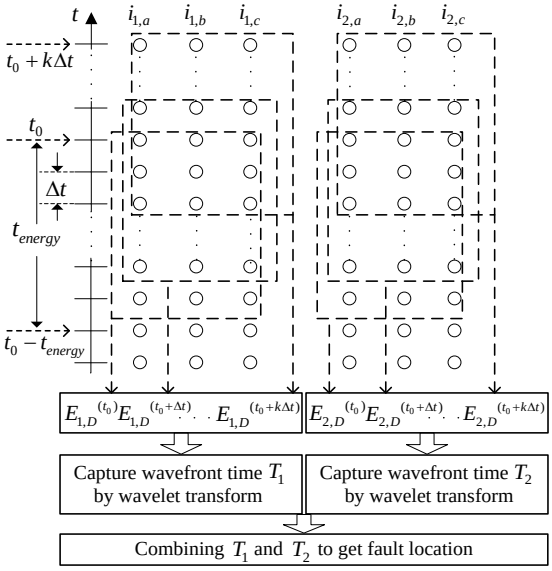

Fig. 5 Calculation process in time domain

V Simulation Results

A 60 Hz, 500 *k*V transmission system, as shown in Fig. 6, has been used for numerical simulations. The compensated line under protection is M1-N1 line, with 83-mile length and 42.4% compensation (0.148 *m*F) installed at N1 side. The bus capacitance is 0.1 μF. The surge impedance of all lines is 250.51 ohm. Three phase currents are measured at two ends of line M1-N1.

According to equation (11) and (12), the computed frequency band is,

$$2.146\ Hz \ll f \ll 12.706\ kHz \quad (18)$$

Here we choose frequency band 1.25 *k*Hz~2.5 *k*Hz, t_{energy} = 3 *m*s, and sampling rate 80 kilo-samples per second (*k*s/s).

Transient waves transmit in two modes, ground mode and line mode, with two different traveling speeds [16]. In this system, the ground mode speed is,

$$v_g = 1/[(L_s + 2L_m)(C_s + 2C_m)]^{1/2} = 2.237 \times 10^8 m/s \quad (19)$$

The line mode speed is,

$$v_l = 1/[(L_s - L_m)(C_s - C_m)]^{1/2} = 2.952 \times 10^8 m/s \quad (20)$$

Thus, we should use the larger speed v_l in (20) for wavefront detections. Next, several events are studied to evaluate the performance of our proposed method.

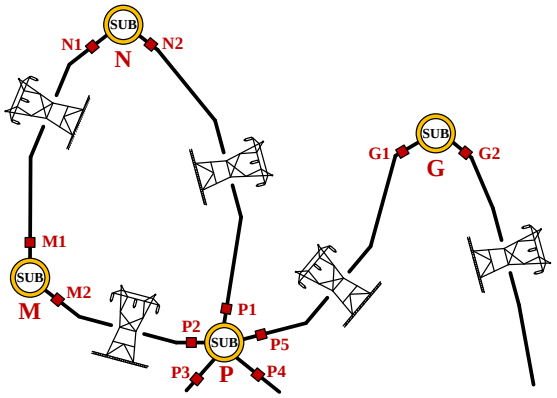

Fig. 6 Numerical simulation system

A. Event 1: Bolt Internal Faults

A 0.01 ohm phase C-N internal fault occurs at 53 miles from side M1. Fig. 7 depicts the energy traveling waves and the wavefront detection enabled by the modulus maxima. From Fig. 7 (a), the energy front occurs at both ends of the transmission line after fault. The modulus maxima in Fig. 7 (b) precisely capture the exact wavefront time difference $\Delta T = 0.275 - 0.15 = 0.125$ *m*s. From equation (16), the relay will correctly trip the line. From equation (17), the fault location is d_{1f} = 52.964 miles. Thus, the method can rapidly trip internal fault and provide accurate fault location in milli-seconds.

B. Event 2: High Impedance Internal Faults

A 2 *k*ohm phase C-N internal fault occurs at 40 miles from side M1. Fig. 8 depicts the energy traveling waves and the wavefront detection enabled by the modulus maxima. We can observe the wavefront time difference is $\Delta T = 0.1875 - 0.2 = -0.0125$*m*s. The relay can rapidly trip this internal fault and precisely locate the fault at d_{1f} = 40.353 miles.

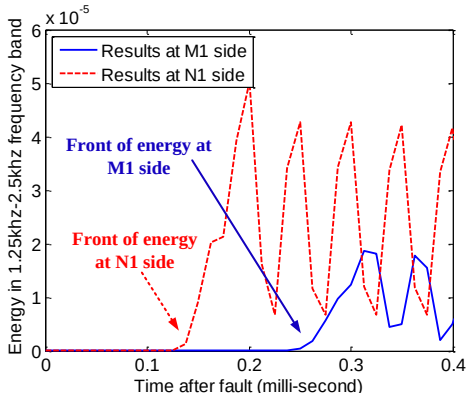

(a) Energy traveling wave

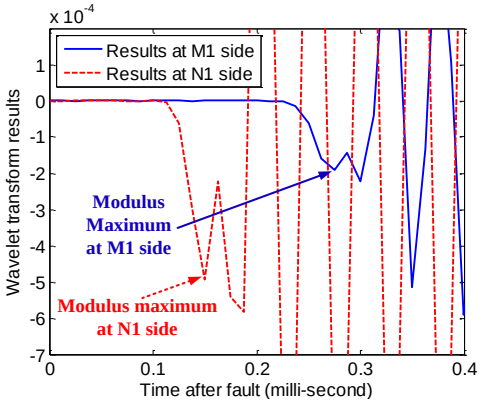

(b) Front detection by the modulus maxima

Fig. 7. Simulation Results - Internal Fault: (C-N fault; impedance:0.01Ω; location: M1-N1 line, M1 side 53 miles)

C. Event 3: Bolt External Faults

A 0.01 ohm phase BC-N external fault occurs inside N2-P1 line, at 20 miles from side N2. Fig. 9 depicts the energy traveling waves and the wavefront detection enabled by the modulus maxima. We can observe the wavefront time difference is $\Delta T = 0.55 - 0.0875 = 0.4625$*m*s. Since it violates equation (16), the relay will not trip.

D. Discussion

(1) MOV/air gap operation. The energy traveling wave algorithm can avoid the MOV/air gap operation since they always operate after faults occur and this algorithm only detects the time of the first wavefront.

(2) Different locations of SCs. From the analysis in Section II, the location of SCs (at the middle of the line or at terminals of the line) will not impact the proper frequency band of the energy traveling wave and the fault detection procedure.

(3) Limitations of the method. The main limitation of the method is that the fault detecting/locating accuracy highly depends on the sampling rate. Related to this issue is that, there exist deadzones for internal faults near terminals, to ensure security of relays during external faults. These disadvantages exist in most of the traveling wave based protection/locating methods. A possible solution is to coordinate with other legacy protection schemes that can detect faults near terminals.

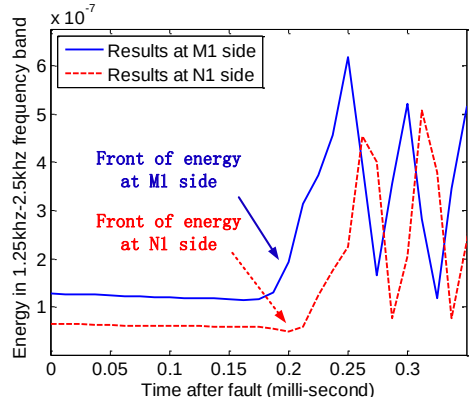

(a) Energy traveling wave

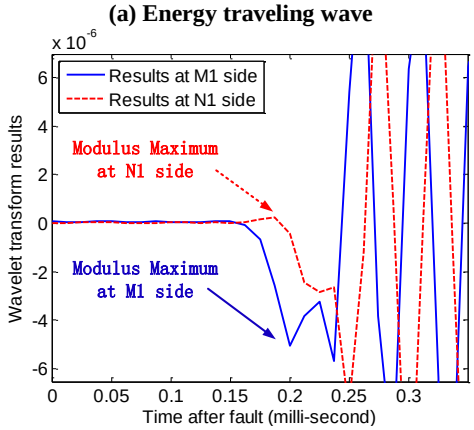

(b) Front detection by the modulus maxima

Fig. 8. Simulation Results – High impedance internal Fault: (C-G fault; impedance: 2 *k*Ω; location: M1-N1 line, M1 side 40 miles)

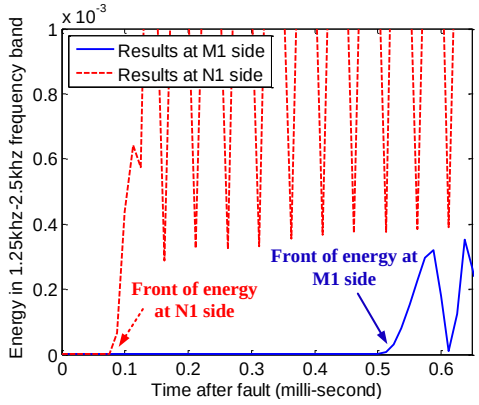

(a) Energy traveling wave

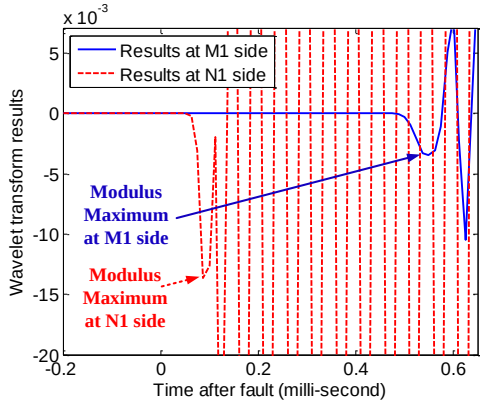

(b) Front detection of by the modulus maxima

Fig. 9. Simulation Results - External Fault: (BC-N fault; impedance:0.01Ω; location: N2-P1 line, N2 side 20 miles)

VI Conclusion

This paper proposed a wavelet transform based energy traveling wave method to accurately determine the location of a fault in series compensated lines and thus to improve protection of these lines. Reflection and refraction properties of transient currents at buses and series capacitors are analyzed. By finding a proper frequency band based on system parameters where attenuation of energy traveling wave is relatively smaller, the simulation results show that the algorithm can rapidly detect and locate internal bolt/high impedance faults. The accurate detection of the fault location makes the protection of the line dependable and secure. The algorithm is not influenced by MOV/air gap operation, and works for different locations of series capacitors. While there exist deadzones for faults near terminals, it can be coordinated with other legacy protection schemes to ensure secure instantaneous trip for the entire length of the line.

References

[1] S. K. Salman, N. Rajoo, and V. Leitloff, "Investigation of the insertion of series capacitors in high voltage on the setting of distance protection," in *Proc.Conf. Develop. Power Syst. Protection*, 2001, pp. 371–374.

[2] T.S.Sidhu, M. Khederzadeh, " Series compensated line protection enhancement by modified pilot relaying schemes," *IEEE Trans. Power Del.*, vol.21, no. 3, pp. 1191-1198, July. 2006.

[3] R. J. Martilla, "Performance of distance relay MHO elements on MOV protected series compensated transmission lines," *IEEE Trans. Power Del.*, vol. 7, pp. 1167–1178, July. 1992.

[4] M. M. Saha, B. Kastenny, E. Rosolowski, and J. Izykowski, "First zone algorithm for protection of series compensated lines," *IEEE Trans. Power Del.*, vol. 16, pp. 200–207, Apr. 2001.

[5] S. He, J. Suonan, Z.Q. Bo, " Integrated Impedance-Based Pilot Protection Scheme for the TCSC-Compensated EHV/UHV Transmission Lines ", *IEEE Trans. Power Del.* , vol. 28, no.2, pp. 835-844, Apr. 2013.

[6] Girgis, A.A., Sallama, A.A., and Karim El-din, A. "An adaptive protection scheme for advanced series compensated (ASC) transmission lines", *IEEE Trans. Power Deliv.*, 1998, 13, pp.414-420.

[7] Reyes-Archundia, E., Moreno-Goytia, E.L. "Analysis of the Effects of a High Power Electronics Controller on Electrical Grids during Faulted and Post-Faulted Conditions Using Wavelets", in *12th Int. Power Electronics Congr. (CIEP)*, 2010, pp 240-245.

[8] Samantaray, S.R., Dash, P.K. "Wavelet packet-based digital relaying for advanced series compensated line". *Gener. Transm. Distrib.*, 2007, 1, 784-792.

[9] B. Bachmann, D. Novosel, D. Hart, Y. Hu, and M. M. Saha, "Application of artificial neural networks for series compensated line protection," in *Proc. Int. Conf. Intelligent Syst. Applicat. Power Syst.*, 1996, pp. 68–73.

[10] Song, Y.H., Johns, A.T., and Xuan, Q.Y. "Artificial neural network based protection scheme for controllable series-compensated EHV transmission lines", *IEE Proc. Gener. Transm. Distrib.*, 1996, 143(6), pp.535-540.

[11] M. Kezunovic, "Smart fault location for smart grid," *IEEE Trans. Smart Grid*, vol. 2, no. 1, pp. 11–22, Mar. 2011.

[12] Ying Zhang, Nengling Tai, and Bin Xu. "Fault Analysis and Traveling-Wave Protection Scheme for Bipolar HVDC Lines", *IEEE Trans. Power Del.* , vol. 27, no. 3, pp. 1583–1591, July. 2012.

[13] Chui, Charles K. *An Introduction to Wavelets*. San Diego: Academic Press, 1992.

[14] Wei Chen, O.P. Malik, Xianggen Yin, Deshu Chen, Zhe Zhang. " Study of Wavelet-Based Ultra High Speed Directional Transmission Line Protection", *IEEE Trans. Power Deliv.* , vol. 18, no. 4, pp. 1134-1139, Oct. 2003.

[15] A.H. Osman, O.P. Malik, "Transmission Line Distance Protection Based on Wavelet Transform", *IEEE Trans. Power Deliv.* , vol. 19, no. 2, pp. 515-523, Apr. 2004.

[16] A.P. Sakis Meliopoulos, *Power System Grounding and Transient: An Introduction.* New York, Marcel Dekker, Inc, 1988, pp.381-391.